

# UCSF

## UC San Francisco Previously Published Works

### Title

Amyloidogenicity, Cytotoxicity, and Receptor Activity of Bovine Amylin: Implications for Xenobiotic Transplantation and the Design of Nontoxic Amylin Variants

### Permalink

<https://escholarship.org/uc/item/7s514576>

### Journal

ACS Chemical Biology, 13(9)

### ISSN

1554-8929

### Authors

Akter, Rehana  
Bower, Rebekah L  
Abedini, Andisheh  
et al.

### Publication Date

2018-09-21

### DOI

10.1021/acscchembio.8b00690

Peer reviewed



Published in final edited form as:

ACS Chem Biol. 2018 September 21; 13(9): 2747–2757. doi:10.1021/acscchembio.8b00690.

## Amyloidogenicity, Cytotoxicity and Receptor Activity of Bovine Amylin; Implications for Xenobiotic Transplantation and the Design of Non-toxic Amylin Variants

Rehana Akter<sup>1</sup>, Rebekah L. Bower<sup>2</sup>, Andisheh Abedini<sup>3</sup>, Ann Marie Schmidt<sup>3</sup>, Debbie L. Hay<sup>2</sup>, Daniel P. Raleigh<sup>1,4,\*</sup>

<sup>1</sup>Department of Chemistry, Stony Brook University, Stony Brook, NY 11794-3400, United States

<sup>2</sup>School of Biological Sciences and Maurice Wilkins Centre for Molecular Biodiscovery, University of Auckland, Auckland, 1142, New Zealand <sup>3</sup>Diabetes Research Program, NYU School of Medicine, 522 First Avenue, New York, NY 10016, United States <sup>4</sup>Institute of Structural and Molecular Biology, University College London, Gower Street, London, WC1E 6BT, United Kingdom

### Abstract

Islet amyloid formation contributes to  $\beta$ -cell death and dysfunction in type-2 diabetes and to the failure of islet transplants. Amylin (Islet amyloid polypeptide, IAPP), a normally soluble 37 residue polypeptide hormone produced in the pancreatic  $\beta$ -cells, is responsible for amyloid formation in type-2 diabetes and is deficient in type-1 diabetes. Amylin normally plays an adaptive role in metabolism and the development of non-toxic, non-amyloidogenic, bioactive variants of human amylin are of interest for use as adjuncts to insulin therapy. Naturally occurring non-amyloidogenic variants are of interest for xenobiotic transplantation and because they can provide clues towards understanding the amyloidogenicity of human amylin. The sequence of amylin is well conserved among species, but sequence differences strongly correlate with *in vitro* amyloidogenicity and with islet amyloid formation *in vivo*. Bovine amylin differs from the human peptide at ten positions and is one of the most divergent among known amylin sequences. We show that bovine amylin oligomerizes, but is not toxic to cultured  $\beta$ -cells and is considerably less amyloidogenic than the human polypeptide and is only a low potency agonist at human amylin-

\*Corresponding Author: Author to whom correspondence should be addressed, DPR; daniel.raleigh@stonybrook.edu; Phone: (631) 632-9547; Fax: (631) 632-7960.

### ASSOCIATED CONTENT

#### Supporting Information

Supporting methods, sequence of amylin from different species (Figure S1), comparison of amyloidogenicity of human amylin and b-amylin deduced by different amyloid prediction programs (Table S1), concentration dependence thioflavin-T kinetics assays of h-amylin and b-amylin (Figure S2), thioflavin-T kinetics assay of bovine amylin in PBS buffer with TEM measurements (Figure S3), photoinduced cross-linking assays showing comparison of oligomeric species distribution in solution (Figure S4), amyloid formation assays of b-amylin in presence of LUV's (Figure S5), comparison of solubility of h-amylin, b-amylin and H18P h-amylin (Figure S6),  $\beta$ -cell toxicity assays at different concentrations (Figure S7), thioflavin-T kinetics assay of h-amylin mutants plotted as absolute fluorescence (Figure S8), amyloid formation assay of H18P h-amylin (Figure S9), comparison of  $T_{50}$  values for variants of human amylin (Figure S10), P18H b-amylin amyloid formation assays (Figure S11), summary of activity data of h-amylin variants (Table S2), activity assays for P18H b-amylin (Figure S12, Table S3), CD spectra of h-amylin, b-amylin, H18P h-amylin and P18H b-amylin (Figure S13 and 14), AGADIR analysis (Figure S15) and MALDI-TOF mass spectra of all peptides (Figure S16).

The authors declare no competing financial interest.

responsive receptors. The bovine sequence contains several non-conservative substitutions relative to human amylin including His to Pro, Ser to Pro and Asn to Lys replacements. The effect of these substitutions is analyzed in the context of wild type human amylin; the results provide insight into their role in receptor activation, the mode of assembly of human amylin and into the design of soluble amylin analogs.

## Keywords

Amylin; Amyloid; Islet Amyloid Polypeptide; Amylin-Receptor; Diabetes;  $\beta$ -cell; Islet Transplantation

$\beta$ -cell death and dysfunction play central roles in the progression of type-2 diabetes. Pancreatic islet amyloid formation by the polypeptide hormone amylin (islet amyloid polypeptide, IAPP) is an important contributing factor.<sup>1</sup> The deposition of islet amyloid also contributes to the failure of islet transplants.<sup>2</sup> Human amylin (h-amylin) is a 37 residue polypeptide hormone that, in its soluble form, plays an adaptive role in metabolism, but aggregates to form pancreatic islet amyloid during the progression of type-2 diabetes.<sup>3-5</sup> The polypeptide is synthesized in the pancreatic  $\beta$ -cells, stored in the insulin secretory granule and released in response to the same stimuli that leads to insulin secretion, h-Amylin, like insulin, is deficient in type-1 diabetes. Non-amyloidogenic variants of h-amylin have been developed for clinical use and one designed analog, Pramlintide (Symlin), has been approved by the FDA.<sup>6</sup> Amylin causes meal-ending satiation and has also been under consideration for treating obesity. Thus, there is significant interest in understanding amylin behavior.

Not all organisms develop islet amyloid *in vivo* and the ability to do so correlates with *in vitro* amyloidogenicity and with the primary sequence of amylin.<sup>7</sup> Amylin is found in all mammals examined and is well conserved, although there are variations. The peptide contains a strictly conserved disulfide bridge between Cys-2 and Cys-7 and a conserved amidated C-terminus (Figure 1). The analysis of inter-species variations in amyloidogenicity can provide clues to the factors that influence the tendency of h-amylin to form amyloid and insight into the mechanism of amyloid formation. Until recently type-2 diabetes has been a disease that affected older humans, thus there was presumably little selective pressure to avoid islet amyloid formation.<sup>8</sup> In contrast, some organisms face naturally metabolically challenging environment such as significant annual weight gain, or a very high fat diet, or a high caloric diet. These are conditions that promote islet amyloid formation in transgenic mice expressing h-amylin. Thus, the analysis of amylin derived from species which face metabolically challenging environments could provide clues towards adaptive strategies, as could the analysis of domestic animals such as pigs and cattle that have been bred to store significant amounts of energy.<sup>9-11</sup> Along these lines, black bear, polar bear and porcine amylin are all non-toxic to  $\beta$ -cells and non-amyloidogenic *in vitro* under standard conditions.<sup>2,9</sup>

Analysis of the amyloidogenicity and cytotoxicity of non-human amylin is also of interest from the perspective of xenobiotic transplantation. Along these lines, porcine islet grafts lead to improved long term glycemic control in laboratory animals while transplantation

with human islet grafts results in only temporary improvement. Porcine amylin is much less amyloidogenic than human amylin and this correlates with the improved glycemic control offered by porcine islet transplantation.<sup>2</sup> Non-amyloidogenic variants of h-amylin are also of interest as potential next generation adjuncts to insulin therapy.<sup>12</sup>

The primary sequence of amylin is highly conserved, but not all species form amyloid *in vivo* and the ability to do so depends on the primary sequence.<sup>7</sup> Rat/mouse amylin (r-amylin) differs from the human peptide at six positions and five of these are located between residues 20 to 29 (Figure S1). Important early work focused on the role of the primary sequence in this region in determining amyloidogenicity.<sup>13</sup> More recent studies have shown that substitutions outside of the 20 to 29 segment can have significant effects on amyloid formation.<sup>14,15</sup> r-Amylin contains three proline residues in the 20-29 region, and this is believed to be an important factor contributing to the non-amyloidogenicity of r-amylin. h-Amylin and bovine amylin (b-amylin) differ at ten positions, four of which are located between residues 20 and 29. These include N22K, F23L, L27F and S29P replacements. N22K and S29P are the least conservative of these and are expected to reduce amyloidogenicity; N22K because it increases the net charge and S29P because Pro residues disrupt  $\beta$ -sheets. A F23L replacement in h-amylin has been shown to slow amyloid formation by a factor of 2 *in vitro*.<sup>16</sup> b-Amylin has several additional charged and proline residues outside of the 20 to 29 region relative to h-amylin (Figure 1). These include non-conservative H18P and N31K replacements as well as an A8E substitution. Overall, b-amylin contains 2 Pro residues and 5 charged residues at neutral pH, while h-amylin contains no Pro residues and 2 or 3 charged residues depending upon the protonation state of His-18.

Although b-amylin is one of the most divergent amylin sequences reported, its ability to form amyloid, its potential toxicity towards  $\beta$ -cells and its activity toward human amylin receptors have not been studied (Figure 1, Figure S1). Reports of diabetes in cattle are rare and have often been linked to bovine viral diarrhea (BVD) and it is not known if cows develop islet amyloid *in vivo* or if bovine amylin is amyloidogenic *in vitro*.<sup>17-19</sup> Here we examine the amyloidogenicity and cytotoxicity of b-amylin and the activity of b-amylin towards multiple amylin-responsive receptors, three subtypes of the h-amylin receptor (AMY) as well as the human calcitonin receptor. We specifically used the CT<sub>(a)</sub> form of the calcitonin receptor in the absence or presence of receptor activity-modifying proteins (RAMPs).

## RESULTS

### Bovine amylin is significantly less amyloidogenic than human amylin.

We analyzed the h-amylin and b-amylin sequences using several standard amyloid prediction programs.<sup>20</sup> These programs employ different methodologies, but we found that all of them agree that b-amylin is less amyloidogenic than h-amylin (Table S1). However, it is important to experimentally evaluate the amyloidogenicity of b-amylin since amyloid prediction programs have been shown to give inconsistent results for other variants of amylin.<sup>21</sup>

We investigated the amyloidogenicity of b-amylin by using thioflavin-T binding fluorescence assays to measure the kinetics of amyloid formation and transmission electron microscopy (TEM) to test for the presence or absence of amyloid fibrils. Thioflavin is a small extrinsic fluorescence dye whose quantum yield increases when bound to amyloid fibrils.<sup>22</sup> The dye provides a convenient assay of amyloid formation kinetics, but can lead to false negatives.<sup>21</sup> Consequently, we used TEM to independently monitor amyloid formation.

First, we studied the ability of b-amylin to form amyloid at pH 7.4 using 20 mM Tris buffer since Tris buffer has been extensively used in biophysical studies of amyloid formation by h-amylin. A typical sigmoidal thioflavin-T fluorescence kinetic curve was observed for h-amylin amyloid formation with a time to reach 50 % of the final fluorescence change,  $T_{50}$ , of 16 h. TEM images revealed dense mats of amyloid fibrils (Figure 2). In contrast, no increase in thioflavin-T fluorescence signal was observed for b-amylin even after 6 days of incubation (Figure 2). TEM images were collected at different time points, and no amyloid fibrils were detected for the b-amylin samples even after 21 days of incubation (Figure 2). We further tested h-amylin and b-amylin at a range of different concentrations. h-Amylin readily formed amyloid at all concentrations tested. In contrast, no amyloid was detected for b-amylin over the time period tested, even at the highest concentration examined (64  $\mu$ M) (Figure S2)

We also compared amyloid formation by h-amylin and b-amylin in phosphate buffered saline (PBS, 10 mM phosphate 140 mM KCl) at pH 7.4. h-Amylin amyloid formation is very sensitive to added salt, as well as the choice of the anion and is faster in PBS relative to Tris.<sup>23</sup> As expected, h-amylin amyloid formation was accelerated in PBS buffer and the  $T_{50}$  decreased to 3 h (Figure S3). In contrast, no significant increase in thioflavin-T fluorescence signal was observed for b-amylin under these conditions, even after 7 days of incubation, and no amyloid fibrils were detected in TEM images of the b-amylin sample (Figure S3).

We next tested if b-amylin forms oligomers. Oligomeric, pre-fibril forms of h-amylin are the most toxic species,<sup>24,25</sup> but nontoxic rat amylin also forms oligomeric species even though it does not form amyloid.<sup>24,26</sup> We use *in situ* photochemical cross-linking followed by detection with SDS-PAGE to probe the distribution of oligomeric forms populated by h-amylin.<sup>24,27</sup> A range of oligomeric species up to hexamers were detected for both the human and bovine polypeptides, providing additional evidence that not all oligomers are toxic (Figure S4).<sup>24</sup>

Interaction with negatively charged membranes is known to promote amyloid formation by h-amylin.<sup>28, 29</sup> Consequently, we tested the ability of large unilamellar vesicles (LUV's) containing 25% of anionic lipid, 1-palmitoyl-2-oleoyl-sn-glycero-3-phosphoL-serine (POPS) and 75% of the zwitterionic lipid 1-palmitoyl-2-oleoyl-sn-glycero-3-phosphocholine (POPC) to promote amyloid formation by b-amylin. As expected, h-amylin rapidly formed amyloid when incubated with these vesicles. In contrast no amyloid formation was detected for the bovine polypeptide even under these strongly amyloid promoting conditions (Figure S5). In summary, we found that b-amylin is significantly less amyloidogenic than h-amylin under all conditions tested. The decreased amyloidogenicity of b-amylin was accompanied by increased solubility relative to h-amylin. The H18P substitution found in b-amylin makes

a significant contribution to the enhanced solubility, but is not solely responsible for the difference between bovine and h-amylin (Figure S6).

### **Bovine amylin is significantly less toxic towards cultured $\beta$ -cells**

We studied the effect of bovine amylin on  $\beta$ -cell viability using rat INS-1/832-13  $\beta$ -cells and Alamar blue reduction assays. INS-1/832-13  $\beta$ -cells are a pancreatic cell line that is widely used for amylin amyloidogenesis toxicity studies. We tested the effects on  $\beta$ -cell viability of 15  $\mu$ M, 22  $\mu$ M and 30  $\mu$ M b-amylin on  $\beta$ -cell viability after 24 h, 48 h, and 84 h of incubation of the peptide on the cells. h-Amylin was used as a positive control. 30  $\mu$ M h-amylin significantly decreased cell viability to 52 % after 24 h while b-amylin did not exhibit any toxicity (Figure 3). A further decrease in cell viability was induced by h-amylin after longer incubation times; cell viability declined to 38 % and 31 % at 48 h and 84 h respectively (Figure S7). In striking contrast, 30  $\mu$ M b-amylin was not toxic, even after 84 h incubation (Figure S7).

### **Bovine amylin weakly activates hCT<sub>(a)</sub> and hAMY<sub>(a)</sub> receptors**

In consideration of the potential value of bovine islet xenografts, it was of interest to determine the bioactivity of bovine amylin at human amylin receptors. The h-amylin receptor is composed of the human calcitonin receptor complexed with a RAMP, this leads to multiple forms of h-amylin receptor.<sup>4</sup> Therefore, the biological activity of b-amylin and h-amylin were measured by analyzing the production of cAMP, a standard assay for amylin receptor activity, at a human calcitonin receptor, hCT<sub>(a)</sub>, and at three different human amylin receptors, hAMY<sub>1(a)</sub>, hAMY<sub>2(a)</sub>, hAMY<sub>3(a)</sub> *in vitro*.<sup>30</sup> Stimulation of cAMP production occurred with b-amylin, however b-amylin was at least 300-fold less potent than h-amylin (Figure 4). Interestingly, b-amylin remained a partial agonist at the hCT<sub>(a)</sub> receptor, only reaching 60% of the E<sub>max</sub> compared to h-amylin while at the hAMY<sub>1(a)</sub> receptor, it was a full agonist. This is likely because we could not use sufficiently high peptide concentrations to achieve a full curve at the calcitonin receptor. A summary of the quantified data is presented in table 1.

### **Mutational analysis of human amylin provided insight into the reduced amyloidogenicity of bovine amylin**

We investigated several point mutants of h-amylin in order to probe the cause of the reduced amyloidogenicity of b-amylin. We tested single point variants of h-amylin corresponding to the four least conservative b-amylin substitutions H18P, N22K, S29P, N31K using thioflavin-T assays and TEM. The Asn to Lys substitutions are unusual non-conservative replacements in amylin and are expected to reduce amyloidogenicity by increasing the net charge on the polypeptide. The consequences of Asn to Lys substitutions on h-amylin formation have not yet been reported. Pro is a well-known disrupter of secondary structure and is not compatible with the classic parallel, in register,  $\beta$ -sheet structures which form the core of amyloid fibrils. Pro 18 is located in a region thought to be important for initial oligomerization during amylin aggregation and a proline at position 18 is a very unusual replacement (Figure S1).<sup>31, 32</sup> The Ser to Pro replacement at position 29 is not found in primates. According to structural models of the h-amylin amyloid fibril, Ser 29 forms key interactions with adjacent residues in the amyloid fibril core and these are presumably

important for fibril structure and stability (Figure 1).<sup>31,33</sup> Thus, a Ser to Pro substitution at position 29 could reduce amyloidogenicity. The S29P replacement is also one of the substitutions found in non-amyloidogenic r-amylin.

All the mutants reduced the rate of amyloid formation and led to lower thioflavin-T intensity, but fibrils were still observed by TEM (Figure 5, Figure S8). H18P h-amylin had the greatest effect. No fibrils were detected in Tris after incubating a 16  $\mu$ M sample for one week, but fibrils were detected for a 32  $\mu$ M sample (Figure S9). The H18P human mutant is also more soluble than wildtype h-amylin, but is less soluble than bovine amylin (Figure S6). The H18P mutant does form oligomers as judged by cross-linking indicating that a non-conservative substitution in this region does not abolish oligomer formation (Figure S4). The cross-linking studies cannot distinguish between the different conformation of oligomers, so it is not possible to deduce if any changes in oligomeric structure correlate with the reduced amyloidogenicity of the H18P mutant. The  $T_{50}$  for N22K h-amylin, S29P h-amylin and N31K h-amylin were about 50 h, 29 h and 32 h respectively, representing approximately 3 to 2-fold increases in  $T_{50}$  under the conditions of these experiments (Figure S10). According to structural models of h-amylin, residues 18 and 22 are in a turn region of the amyloid fibril while residues 29 and 31 are in the C-terminal  $\beta$ -sheet structure and make key interactions with adjacent residues in the core of the amyloid fibril (Figure 1).<sup>31,33</sup>

While the proline at position 18 plays a major role in reducing the amyloidogenicity of b-amylin, it is not solely responsible for the decrease. A P18H mutant of b-amylin did not form amyloid as judged by thioflavin-T and TEM measurements, after 1 week incubation in Tris at pH 7.4 (Figure S11). Our mutational analysis indicates that residues in the proposed turn region have more effect on amyloidogenicity than at least some of the sites in the putative C-terminal  $\beta$ -strand of the amyloid fibril.

### **Mutational analysis of human amylin aids in understanding reduced $\beta$ -cell toxicity of bovine amylin**

We studied the effect of H18P, N22K, and S29P mutants of h-amylin on rat INS-1  $\beta$ -cells toxicity. Cell viability was measured using 30  $\mu$ M of each peptide after 24 h and 48 h incubation (Figure 6). The H18P mutant was the least toxic of the three variants. After 24 h of incubation, cell viability decreased only by 17 % and after 48 h by about 30 %. 24 h incubation with the N22K variant reduced cell viability by 60 % and after 48 h incubation by about 73 %. Similarly, for the S29P variant, cell viability was decreased by 65 % and 71 % after 24 h and 48 h incubation respectively. Analysis of the toxicity profiles indicates that proline at position 18 has a substantial effect on the reduction of b-amylin toxicity.

### **Mutational analysis of human amylin to understand the decreased potency of bovine amylin at hAMY<sub>1(a)</sub> and hCT<sub>(a)</sub> receptors**

To understand the drastic potency reduction of the b-amylin peptide at hCT<sub>(a)</sub> and hAMY<sub>1(a)</sub> receptors, the same four h-amylin peptides with single point mutations from the bovine sequence were analyzed for their activity at amylin-responsive receptors (Figure 7 and Table S2). The peptide substitution with the largest impact on h-amylin potency was H18P, resulting in potency reductions of 7 and 20-fold at the hCT<sub>(a)</sub> and hAMY<sub>1(a)</sub> receptors,

respectively. Despite the reductions in potency, this analog remained a full agonist at both receptors. The S29P, N22K and N31K substitutions were well tolerated, with no detrimental impact on receptor activity at either receptor, despite the fact they are non-conservative replacements. The data are summarized in table S2. In order to further test the role of the H18P substitution in reducing activity we examined a P18H b-amylin mutant at the hCT<sub>(a)</sub> and hAMY<sub>1(a)</sub> receptors. Replacement of the bovine residue P18 with the human His residue significantly increased the activity at both receptors by almost 50 and 40 fold respectively (Figure S12, Table S3). However, the activity of the mutant was still less than that of h-amylin, indicating that other substitutions in b-amylin also contribute to decrease activity towards h-amylin receptors.

## DISCUSSION

The results presented here clearly show that b-amylin is considerably less amyloidogenic than h-amylin, more soluble, less toxic to  $\beta$ -cells and is weakly potent at mutant h-amylin and calcitonin receptors. The considerable reduction in activity towards h-amylin responsive receptors indicates that bovine islets are not suitable candidates for xenobiotic transplantation. The decreased amyloidogenicity and non-toxic nature of b-amylin is consistent with the hypothesis that reducing the potential to form islet amyloid may be a response to metabolically challenging environment.<sup>9</sup>

The mutational analysis indicates that the His 18 to Pro substitution plays a major role, but is not solely responsible for the reduced amyloidogenicity, reduced toxicity and reduced receptor activity of b-amylin. Analysis of the h-amylin mutants provides some insight into amyloid formation by wild type h-amylin amyloid formation. h-Amylin has a tendency to populate helical  $\phi$ ,  $\psi$  i.e. the region of residues 8 to 22.<sup>34</sup> One model of h-amylin amyloid formation posits that the process is initially driven by association of transiently populated helical conformers of amylin where the helical structure is localized in the N-terminal half to two-thirds of the molecule. This in turn would generate a high local concentration of the C-terminal region of the peptide which promotes the formation of the cross  $\beta$ -sheet structure.<sup>35</sup> Residue 18 is in a region proposed to be important for the initial helical oligomerization<sup>32,35,36</sup> and proline is energetically very unfavorable in a  $\alpha$ -helix. The reduced rate of amyloid formation is consistent with this region playing a role in aggregation despite the fact that it falls outside of the putative amyloidogenic core of h-amylin. However, the H18P mutant does form amyloid, arguing that helical structure at or adjacent to His-18 is not a strict requirement for h-amylin amyloid formation. It is difficult to make more definitive conclusions about the role of helical structure from a comparison of b-amylin and h-amylin. CD spectra of b-amylin and the h-amylin exhibit low helicity in buffer, but adopt more helicity in TFE (Figure S13). The H18P substitution reduces the helicity of the human peptide in 30% TFE as judged by the ratio of intensity at 222 nm to the intensity at 208 nm (Figure S14). Conversely the P18H substitution in the bovine increases helicity by the same criteria (Figure S14). However, the effects are relatively modest and suggest that the H18P replacement does not abolish the tendency to sample helical  $\phi$ ,  $\psi$  angles for many of the other residues in h-amylin. Consistent with this hypothesis, calculations using the AGADIR program argue that the H18P replacement does not impact the helical propensity up to residue 17 (Figure S15).<sup>37</sup> b-Amylin also contain an Ala at residue 17 while h-Amylin

contains a Val. Val has low helical propensity while Ala has a high helical propensity. Thus, the two peptides each contain one substitution that reduces helical propensity relative to each other and one that increases helical propensity.

The transition from oligomers to  $\beta$ -sheet rich amyloid fibrils has been proposed to occur through the transient formation of parallel, in register, intermolecular,  $\beta$ -sheet structure localized near Phe-23 within the 20-29 region of hIAPP.<sup>38</sup> This structure develops during the lag phase and serves to align the peptide stands in register; the structure is then disrupted during the transition to the final fibril state and the development of cross- $\beta$  structure in other regions of the molecule. This model predicts that substitutions within the turn region should influence the kinetics of amyloid fibril formation even if the substitutions are at sites that are not part of the cross- $\beta$  core of the fibril. The exact identity of the residues, participating in the transient  $\beta$ -sheet are not yet known, but the sensitivity of the kinetics of amyloid formation to substitutions at residue 22 is broadly consistent with this model, however the model makes no prediction about residues outside of this region.

The analysis of the N22K and N31K variants shows that charged residues as well as proline substitutions make important contributions to reducing amyloidogenicity, consistent with earlier studies that examined H18R and S20K variants of h-amylin.<sup>39, 40</sup> That work together with the present study indicates the substitution with charged residues at key locations is a straight forward strategy for reducing amyloidogenicity.

It is interesting that despite being 73% identical with h-amylin, b-amylin had such a substantial reduction in receptor potency. This is likely due to the fact that we used human rather than bovine receptors. There is little information about amylin activity across species, although h-amylin is reported to be active at porcine calcitonin and amylin receptors.<sup>41</sup> It is not known if porcine amylin is active at human receptors. Rat amylin and h-amylin have similar potency at their respective receptors<sup>42</sup> and r-amylin is 78% identical to b-amylin.

It is evident from the functional data that the proline at position 18 in place of the native histidine contributes towards the reduced potency. Adding a proline at this position may interfere with important side-chain interactions made by the basic histidine side chain of h-amylin or may unfavorably alter the secondary structure of the peptide. There are no structures of amylin bound to an amylin responsive receptor.<sup>43, 44</sup> Amylin is a member of the CGRP family of polypeptide hormones and these molecules are proposed to contain an amphiphilic helix located in the first  $\frac{1}{2}$  to  $\frac{2}{3}$  of the molecule that starts after the disulfide, and which may be important for receptor binding. Structures of fragments of CGRP, adrenomedullin and calcitonin bound to the extracellular domain of these receptors show that the C terminal portion of the peptides in this family contain a turn. Models of the C-terminal portion of amylin bound to amylin receptors suggests that amylin binds in a similar manner<sup>45</sup> and it is likely that the peptide helix binds to the extracellular loops or transmembrane bundle of the receptor. A Pro at position 18 could significantly destabilize ordered structure in this region of the peptide, potentially rationalizing the significant effect of the H18P substitution. A detailed analysis will require a high resolution structure of h-amylin bound to its receptor. Interestingly, in every other species of amylin, the residue at position 18 is a strongly conserved basic arginine or histidine only deviating in the bovine

sequence (Figure S1). Conversely, a proline substitution at position 29 in place of the native serine of h-amylin had no significant effect on peptide potency. This residue is a proline apart from humans, monkeys, macaques, and baboons which possess a serine, suggesting that prolines are relatively well conserved here and do not impose unfavorable structure disruptions at the peptide-receptor interface. This was perhaps expected as both rat amylin and pramlintide also possess a proline at position 29 and are either equipotent or more potent than h-amylin at human amylin receptors, respectively.

Two other well-tolerated substitutions are the very non-conservative N22K and N31K replacements. Prior work has shown that *in vitro* glycosylation of h-amylin at position N22 or N31 did not eliminate *in vitro* receptor activity and a N31A substitution had only a small effect.<sup>46, 47</sup> Taken together, that work and the present study reveals that h-amylin is remarkably tolerant to substitution at these sites; neither increased bulk induced by glycosylation, nor substitution of a charged residue has a major impact. Thus, these sites are strong candidates for modification to develop less amyloidogenic, but active variants of h-amylin. Replacing asparagine residues should have the added benefit of reducing potential susceptibility to deamidation.<sup>48, 49</sup>

The data presented here show that the bovine polypeptide, is not a suitable candidate for therapeutic use given its low potency towards human amylin receptors. The non-conservative H18P replacement makes a major contribution to the reduced potency; highlighting the importance of this region for polypeptide- receptor interactions. In contrast, the minimal effect on activity deduced for the N22K, S29P and N31K replacements, highlights the tolerance of h-amylin to substitutions in this region of the molecule. Thus, targeting residues in this region is likely to be a fruitful approach for designing amylin variants with lower propensity to aggregate and increased solubility, but which retain biological activity. Of particular interest in this regard is the replacement of Asn-22 and /or Asn-31 with charged residues. Asn substitutions have not yet been incorporated in reported soluble analogs of h-amylin.<sup>6, 12</sup> Of course other strategies to design h-Amylin agonists can prove valuable as well.<sup>50</sup>

## METHODS

### Peptide Synthesis and Purification:

Peptides were synthesized on a 0.1 mmol scale using a CEM Liberty automated microwave peptide synthesizer as described (Supporting methods). Fmoc protected pseudoproline (Oxazolidine) dipeptide derivatives were used to facilitate the synthesis.<sup>25</sup> The oxidized peptides were purified via reversed-phase HPLC using a C18 preparative column (Supporting methods). The purity of the peptides was confirmed by reversed-phase HPLC using a C18 analytical column. Only a single peak was observed in each HPLC trace. The molecular weight of the purified oxidized peptides were confirmed by MALDI-TOF MS: h-amylin expected, 3903.3; observed 3903.3; bovine amylin, expected, 3906.5; observed, 3906.4; H18P h-amylin, expected 3866.3; observed, 3865.9; S29P h-amylin expected, 3913.4; observed, 3914.5; N22K h-amylin, expected 3917.4; observed 3917.6; N31K h-amylin expected 3917.4; observed 3917.4; P18H b-amylin expected 3946.5; observed

3946.4. No deletion peptides were detected nor were any higher molecular weight adducts observed (Figure S16).

#### **Sample Preparation:**

A 0.5 mM peptide stock solution in 100% HFIP was prepared from the dry peptide. Aliquots were filtered through a 0.22  $\mu\text{m}$  Millex syringe-driven membrane filter. The concentration of the stock solution was determined by measuring the UV absorbance at 280 nm. Desired amounts of peptide stock solution were aliquoted and freeze dried to remove HFIP.

#### **Large Unilamellar Vesicles (LUV's) Preparation:**

1-palmitoyl-2-oleoyl-sn-glycero-3-phosphoL-serine (POPS) and 1-palmitoyl-2-oleoyl-sn-glycero-3-phosphocholine (POPC) were obtained from Avanti Polar Lipids. LUV's were prepared from a 25: 75 mixtures of POPS and POPC as described.<sup>29</sup> The effective diameter of the LUV's were confirmed by using dynamic light scattering (DLS). LUV's were freshly prepared before the experiments and final concentration of LUV's was 400  $\mu\text{M}$ .

#### **Fluorescence Amyloid Assays:**

Thioflavin-T binding fluorescence assays were conducted using a Beckman Coulter DTX 880 Multimode Detector plate reader and a Spectramax Gemini EM plate reader (Supporting methods).

#### **Transmission Electron Microscopy:**

TEM images were recorded using an FEI Bio TwinG<sup>2</sup> Transmission Electron Microscope at the central microscopy center at Stony Brook University. 18  $\mu\text{L}$  of peptide solution was taken at the end of the kinetic runs. Samples were blotted on a carbon-coated formvar 300-mesh copper grid for 1 min and then negatively stained with 2% uranyl acetate for 1 min. Images were taken at a 68,000X magnification and 100 nm under focus.

#### **Cytotoxicity Assays:**

Experiments were conducted as described<sup>24</sup> using Alamar Blue assays to assess  $\beta$ -cell viability (Supporting methods).

#### **Cell Culture and Transient Transfections:**

Cos-7 cells were cultured and transfected for receptor activity assays as previously described.<sup>51</sup> Transient transfections were carried out using polyethyleneimine (PEI) as described previously<sup>51</sup> and maintained at 37°C in a humidified 95% air/5% CO<sub>2</sub> incubator for 36 – 48 h. All DNA constructs used in these experiments were in pcDNA3.1 vectors. The insert-negative human CTR with leucine at the polymorphic amino acid position 447 with an N-terminal haemagglutinin (HA) tag (HA-hCTR), myc-tagged hRAMP1, FLAG tagged RAMP2 and untagged RAMP2 were utilized in these experiments.<sup>47</sup>

#### **cAMP Assays:**

Measurement of intracellular cAMP was achieved using a time-resolved fluorescent resonance energy transfer assay (LANCER cAMP assay, PerkinElmer), similar to the

previously described Alphascreen assay,<sup>52</sup> with minor modifications (Supporting methods). Plates were read after an overnight incubation on an Envision plate reader. A standard curve was included in each experiment to ensure accurate quantification of cAMP.

### Data Analysis for Receptor Assays

Data are derived from at least three independent experiments for statistical analysis and all experiments were performed with two or three technical replicates. Quantification of cAMP was obtained from a standard curve included in each experiment and plotted using the software GraphPad Prism 6.0 (GraphPad Software Inc, San Diego, CA, USA) with a non-linear regression 3-parameter logistic equation with a Hill slope of 1 to determine the  $PEC_{50}$ . The  $pEC_{50}$  values from the fits were combined from different experimental days and statistically tested for difference from the WT peptide using the Student's t-test with statistical significance defined as \*  $p < 0.05$ , \*\*  $p < 0.01$ , \*\*\*  $p < 0.001$ . Due to variability in amount of cAMP produced between experimental days, data were normalized to the control peptide for each experiment to obtain  $E_{max}$  values. For each analogue, data were normalized to the maximum ( $E_{max}$ ) and minimum ( $E_{min}$ ) responses of h-amylin. Normalized data for each experiment were combined and statistically tested for differences between analogs and the control h-amylin of b-amylin peptide by an unpaired Students t-test with statistical significance defined as \*  $p < 0.05$ , \*\*  $p < 0.01$ , \*\*\* $p < 0.001$ .

### Circular Dichroism Experiments:

Far UV CD experiments were conducted using an Applied Photophysics Chirascan circular dichroism spectrophotometer (Supporting methods).

### Solubility Assays:

Dry peptides were dissolved in PBS buffer containing 10 mM phosphate buffer with 140 mM KCl at pH 7.4 at 0.5 mM and 1 mM initial concentrations. Each sample was then centrifuged after 7 days incubation in buffer at 25 °C without stirring using a Beckman Coulter Microfuge 22R centrifuge at 24 °C for 20 min ( $1.75 \times 10^4$  g). The apparent solubility of the peptides was measured by measuring the absorbance of the supernatant of each solution at 280 nm using a Beckman Coulter DEI 730 UV/Vis spectrophotometer. Each peptide has a single Tyr, three Phe residues, and a disulfide bond and no Trp therefore the extinction coefficients at 280 nm is identical.

### Photochemical Induced Cross-linking Assays:

Photochemical cross-linking reactions were conducted using Tris(bipyridyl)Ru(II) in presence of ammonium persulfate and analyzed as described<sup>24</sup> (Supporting methods).

### Supplementary Material

Refer to Web version on PubMed Central for supplementary material.

## ACKNOWLEDGEMENTS

We thank members of the Raleigh and Hay groups for helpful discussions. We thank Z. Ridgway for providing the S29P h-amylin peptide and experimental data collected with this peptide, as well as for help with the cross-linking studies and M. Li for help with the LUV studies.

### Funding

This work was supported by grants from the United States Public Health National Institutes of Health, GM078114, to D. P. R. and American Heart Association (17SDG33410350, to AA and from the Marsden Fund, Royal Society of New Zealand to D.L.H.

## REFERENCES:

- (1). Cao P, Marek P, Noor H, Patsalo V, Tu LH, Wang H, Abedini A, and Raleigh DP (2013) Islet amyloid: from fundamental biophysics to mechanisms of cytotoxicity, *FEBS Lett* 587, 1106–1118. [PubMed: 23380070]
- (2). Potter KJ, Abedini A, Marek P, Klimek AM, Butterworth S, Driscoll M, Baker R, Nilsson MR, Warnock GL, Oberholzer J, Bertera S, Trucco M, Korbitt GS, Fraser PE, Raleigh DP, and Verchere CB (2010) Islet amyloid deposition limits the viability of human islet grafts but not porcine islet grafts, *Proc. Natl. Acad. Sci. U. S. A* 107, 4305–4310. [PubMed: 20160085]
- (3). Akter R, Cao P, Noor H, Ridgway Z, Tu LH, Wang H, Wong AG, Zhang X, Abedini A, Schmidt AM, and Raleigh DP (2016) Islet amyloid polypeptide: structure, function, and pathophysiology, *J. Diabetes Res* 2016, 2798269. [PubMed: 26649319]
- (4). Bower RL, and Hay DL (2016) Amylin structure-function relationships and receptor pharmacology: implications for amylin mimetic drug development, *Br. J. Pharmacol* 173, 1883–1898. [PubMed: 27061187]
- (5). Hay DL, Chen S, Lutz TA, Parkes DG, and Roth JD (2015) Amylin: pharmacology, physiology, and clinical potential, *Pharmacol. Rev* 67, 564–600. [PubMed: 26071095]
- (6). Fineman MS, Koda JE, Shen LZ, Strobel SA, Maggs DG, Weyer C, and Kolterman OG (2002) The human amylin analog, pramlintide, corrects postprandial hyperglucagonemia in patients with type-I diabetes, *Metabolism* 51, 636–641. [PubMed: 11979398]
- (7). Westermark P, Andersson A, and Westermark GT (2011) Islet amyloid polypeptide, islet amyloid, and diabetes mellitus, *Physiol. Rev* 91, 795–826. [PubMed: 21742788]
- (8). International Diabetes Foundation Atlas. (2017) <http://diabetesatlas.org/resources/2017-atlas.html>.
- (9). Akter R, Abedini A, Ridgway Z, Zhang XX, Kleinberg J, Schmidt AM, and Raleigh DP (2017) Evolutionary adaptation and amyloid formation: does the reduced amyloidogenicity and cytotoxicity of ursine amylin contribute to the metabolic adaptation of bears and polar bears?, *Isr. J. Chem* 57, 750–761. [PubMed: 29955200]
- (10). Gerstein HC, and Waltman L (2006) Why don't pigs get diabetes? Explanations for variations in diabetes susceptibility in human populations living in a diabetogenic environment, *Can. Med. Assoc. J* 174, 25–26. [PubMed: 16389231]
- (11). Qasim A, Turcotte M, de Souza RJ, Samaan MC, Champredon D, Dushoff J, Speakman JR, and Meyre D (2018) On the origin of obesity: identifying the biological, environmental and cultural drivers of genetic risk among human populations, *Obes. Rev* 19, 121–149. [PubMed: 29144594]
- (12). Wang H, Abedini A, Ruzsicska B, and Raleigh DP (2014) Rationally designed, nontoxic, nonamyloidogenic analogues of human islet amyloid polypeptide with improved solubility, *Biochemistry* 53, 5876–5884. [PubMed: 25140605]
- (13). Westermark P, Engstrom U, Johnson KH, Westermark GT, and Betsholtz C (1990) Islet amyloid polypeptide-pinning amino-acid-residues linked to amyloid fibril formation, *Proc. Natl. Acad. Sci. U. S. A* 87, 5036–5040. [PubMed: 2195544]
- (14). Green J, Goldsbury C, Mini T, Sunderji S, Frey P, Kistler J, Cooper G, and Aebi U (2003) Full-length rat amylin forms fibrils following substitution of single residues from human amylin, *J. Mol. Biol* 326, 1147–1156. [PubMed: 12589759]

- (15). Abedini A, and Raleigh DP (2006) Destabilization of human IAPP amyloid fibrils by proline mutations outside of the putative amyloidogenic domain: is there a critical amyloidogenic domain in human IAPP?, *J. Mol. Biol* 355, 274–281. [PubMed: 16303136]
- (16). Tu LH, and Raleigh DP (2013) Role of aromatic interactions in amyloid formation by islet amyloid polypeptide, *Biochemistry* 52, 333–342. [PubMed: 23256729]
- (17). Deepa PM, Dimri U, Jhambh R, Yatoo MI, and Sharma B (2015) Alteration in clinico-biochemical profile and oxidative stress indices associated with hyperglycaemia with special reference to diabetes in cattle—a pilot study, *Trop. Anim. Health. Pro* 47, 103–109.
- (18). Clark Z (2003) Diabetes mellitus in a 6-month-old Charolais heifer calf, *Can. Vet. J* 44, 921–922. [PubMed: 14664356]
- (19). Tajima M, Yuasa M, Kawanabe M, Taniyama H, Yamato O, and Maeda Y (1999) Possible causes of diabetes mellitus in cattle infected with bovine viral diarrhoea virus, *J. Vet. Med B* 46, 207–215.
- (20). Ahmed AB, and Kajava AV (2013) Breaking the amyloidogenicity code: methods to predict amyloids from amino acid sequence, *FEBS Lett* 587, 1089–1095. [PubMed: 23262221]
- (21). Wong AG, Wu C, Hannaberry E, Watson MD, Shea JE, and Raleigh DP (2016) Analysis of the amyloidogenic potential of pufferfish (*Takifugu rubripes*) islet amyloid polypeptide highlights the limitations of thioflavin-T assays and the difficulties in defining amyloidogenicity, *Biochemistry* 55, 510–518. [PubMed: 26694855]
- (22). LeVine H (1999) Quantification of beta-sheet amyloid fibril structures with thioflavin-T, *Methods Enzymol* 309, 274–284. [PubMed: 10507030]
- (23). Marek PJ, Patsalo V, Green DF, and Raleigh DP (2012) Ionic strength effects on amyloid formation by amylin are a complicated interplay among Debye screening, ion selectivity, and hofmeister effects, *Biochemistry* 51, 8478–8490. [PubMed: 23016872]
- (24). Abedini A, Plesner A, Cao P, Ridgway Z, Zhang J, Tu LH, Middleton CT, Chao B, Sartori DJ, Meng F, Wang H, Wong AG, Zanni MT, Verchere CB, Raleigh DP, and Schmidt AM (2016) Time-resolved studies define the nature of toxic IAPP intermediates, providing insight for anti-amyloidosis therapeutics, *Elife* 5, 10.7554/eLife.12977.
- (25). Abedini A, Cao P, Plesner A, Zhang JH, He ML, Derk J, Patil SA, Rosario R, Lonier J, Song F, Koh H, Li HL, Raleigh DP, and Schmidt AM (2018) RAGE binds preamyloid IAPP intermediates and mediates pancreatic beta cell proteotoxicity, *J. Clin. Invest* 128, 682–698. [PubMed: 29337308]
- (26). Young LM, Cao P, Raleigh DP, Ashcroft AE, and Radford SE (2014) Ion mobility spectrometry-mass spectrometry defines the oligomeric intermediates in amylin amyloid formation and the mode of action of inhibitors, *J. Am. Chem. Soc* 136, 660–670. [PubMed: 24372466]
- (27). Bitan G, and Teplow DB (2004) Rapid photochemical cross-linking - a new tool for studies of metastable, amyloidogenic protein assemblies, *Acc. Chem. Res* 37, 357–364. [PubMed: 15196045]
- (28). Hebda JA, and Miranker AD (2009) The interplay of catalysis and toxicity by amyloid intermediates on lipid bilayers: insights from type II diabetes, *Annu. Rev. Biophys* 38, 125–152. [PubMed: 19416063]
- (29). Zhang XX, St Clair JR, London E, and Raleigh DP (2017) Islet amyloid polypeptide membrane interactions: effects of membrane composition, *Biochemistry* 56, 376–390. [PubMed: 28054763]
- (30). Hay DL, Christopoulos G, Christopoulos A, Poyner DR, and Sexton PM (2005) Pharmacological discrimination of calcitonin receptor: receptor activity-modifying protein complexes, *Mol. Pharmacol* 67, 1655–1665. [PubMed: 15692146]
- (31). Wiltzius JW, Sievers SA, Sawaya MR, Cascio D, Popov D, Riekel C, and Eisenberg D (2008) Atomic structure of the cross-beta spine of islet amyloid polypeptide (amylin), *Protein Sci* 17, 1467–1474. [PubMed: 18556473]
- (32). Gilead S, Wolfenson H, and Gazit E (2006) Molecular mapping of the recognition interface between the islet amyloid polypeptide and insulin, *Angew. Chem. Int. Edit* 45, 6476–6480.
- (33). Luca S, Yau WM, Leapman R, and Tycko R (2007) Peptide conformation and supramolecular organization in amylin fibrils: constraints from solid-state NMR, *Biochemistry* 46, 13505–13522. [PubMed: 17979302]

- (34). Williamson JA, and Miranker AD (2007) Direct detection of transient alpha-helical states in islet amyloid polypeptide, *Protein Sci* 16, 110–117. [PubMed: 17123962]
- (35). Abedini A, and Raleigh DP (2009) A critical assessment of the role of helical intermediates in amyloid formation by natively unfolded proteins and polypeptides, *Protein Eng. Des. Sel* 22, 453–459. [PubMed: 19596696]
- (36). Wiltzius JJW, Sievers SA, Sawaya MR, and Eisenberg D (2009) Atomic structures of IAPP (amylin) fusions suggest a mechanism for fibrillation and the role of insulin in the process, *Protein Sci* 18, 1521–1530. [PubMed: 19475663]
- (37). Munoz V, and Serrano L (1994) Elucidating the folding problem of helical peptides using empirical parameters, *Nat. Struct. Biol* 1, 399–409. [PubMed: 7664054]
- (38). Buchanan LE, Dunkelberger EB, Tran HQ, Cheng PN, Chiu CC, Cao P, Raleigh DP, de Pablo JJ, Nowick JS, and Zanni MT (2013) Mechanism of IAPP amyloid fibril formation involves an intermediate with a transient beta-sheet, *Proc. Natl. Acad. Sci. U. S. A* 110, 19285–19290. [PubMed: 24218609]
- (39). Cao P, Tu LH, Abedini A, Levsh O, Akter R, Patsalo V, Schmidt AM, and Raleigh DP (2012) Sensitivity of amyloid formation by human islet amyloid polypeptide to mutations at residue 20, *J. Mol. Biol* 421, 282–295. [PubMed: 22206987]
- (40). Jha S, Snell JM, Sheftic SR, Patil SM, Daniels SB, Kolling FW, and Alexandrescu AT (2014) pH dependence of amylin fibrillization, *Biochemistry* 53, 300–310. [PubMed: 24377660]
- (41). Kikumoto K, Katafuchi T, and Minamino N (2003) Specificity of porcine calcitonin receptor and calcitonin receptor-like receptor in the presence of receptor-activity-modifying proteins, *Hypertens. Res* 26, S15–S23. [PubMed: 12630807]
- (42). Bailey RJ, Walker CS, Ferner AH, Loomes KM, Prijic G, Halim A, Whiting L, Phillips AR, and Hay DL (2012) Pharmacological characterization of rat amylin receptors: implications for the identification of amylin receptor subtypes, *Br. J. Pharmacol* 166, 151–167. [PubMed: 22014233]
- (43). Johansson E, Hansen JL, Hansen AMK, Shaw AC, Becker P, Schaffer L, and Reedtz-Runge S (2016) Type II turn of receptor-bound salmon calcitonin revealed by X-ray crystallography, *J. Biol. Chem* 291, 13689–13698. [PubMed: 27189946]
- (44). Booe JM, Walker CS, Barwell J, Kuteyi G, Simms J, Jamaluddin MA, Warner ML, Bill RM, Harris PW, Brimble MA, Poyner DR, Hay DL, and Pioszak AA (2015) Structural basis for receptor activity-modifying protein-dependent selective peptide recognition by a G protein-coupled receptor, *Mol. Cell* 58, 1040–1052. [PubMed: 25982113]
- (45). Lee SM, Hay DL, and Pioszak AA (2016) Calcitonin and amylin receptor peptide interaction mechanisms. Insights into peptide-binding modes and allosteric modulation of the calcitonin receptor by receptor activity-modifying proteins, *J. Biol. Chem* 291, 8686–8700. [PubMed: 26895962]
- (46). Kowalczyk R, Brimble MA, Tomabechi Y, Fairbanks AJ, Fletcher M, and Hay DL (2014) Convergent chemoenzymatic synthesis of a library of glycosylated analogues of pramlintide: structure-activity relationships for amylin receptor agonism, *Org. Biomol. Chem* 12, 8142–8151. [PubMed: 25030939]
- (47). Bower RL, Yule L, Rees TA, Deganutti G, Hendrikse ER, Harris PWR, Kowalczyk R, Ridgway Z, Wong AG, Swierkula K, Raleigh DP, Pioszak AA, Brimble MA, Reynolds CA, Walker CS, and Hay DL (2018) Molecular signature for receptor engagement in the metabolic peptide hormone amylin, *ACS Pharmacol. Transl. Sci* DOI: 10.1021/acsptsci.8b00002, Article ASAP.
- (48). Dunkelberger EB, Buchanan LE, Marek P, Cao P, Raleigh DP, and Zanni MT (2012) Deamidation accelerates amyloid formation and alters amylin fiber structure, *J. Am. Chem. Soc* 134, 12658–12667. [PubMed: 22734583]
- (49). Wakankar AA, and Borchardt RT (2006) Formulation considerations for proteins susceptible to asparagine deamidation and aspartate isomerization, *J. Pharm. Sci* 95, 2321–2336. [PubMed: 16960822]
- (50). Mack CM, Soares CJ, Wilson JK, Athanacio JR, Turek VF, Trevaskis JL, Roth JD, Smith PA, Gedulin B, Jodka CM, Roland BL, Adams SH, Lwin A, Herich J, Laugero KD, Vu C, Pittner R, Paterniti JR, Hanley M, Ghosh S, and Parkes DG (2010) Davalintide (AC2307), a novel amylin-

mimetic peptide: enhanced pharmacological properties over native amylin to reduce food intake and body weight, *Int. J. Obes* 34, 385–395.

- (51). Bailey RJ, and Hay DL (2006) Pharmacology of the human CGRP1 receptor in Cos 7 cells, *Peptides* 27, 1367–1375. [PubMed: 16375989]
- (52). Gingell JJ, Qi T, Bailey RJ, and Hay DL (2010) A key role for tryptophan 84 in receptor activity-modifying protein 1 in the amylin 1 receptor, *Peptides* 31, 1400–1404. [PubMed: 20347903]

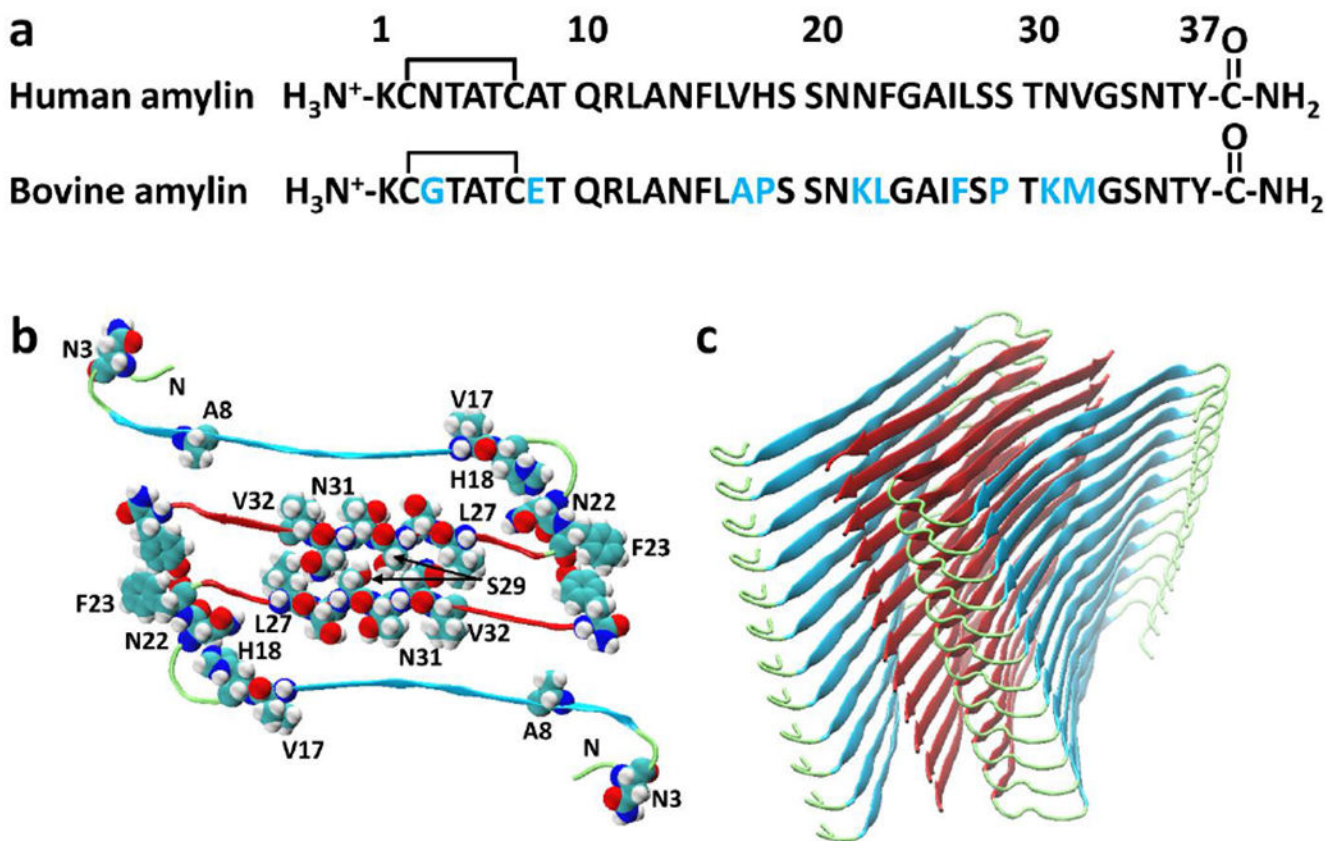


**Figure 1:**

(a) Primary sequence of human and bovine amylin. The polypeptides have an amidated C-terminus and an intramolecular disulfide bond between residue 2 and 7. Residues in bovine amylin which differ from those in human amylin are colored blue. (b) A top down view of a model of the human amylin amyloid fibril based on crystal structures of small fragments of h-amylin.<sup>31</sup> Residues in bovine amylin that differ from human amylin are shown in space filling format together with some of the key residues that they interact with. (c) A side view of the structure in ribbon format. The N-terminal  $\beta$ -strand in each monomer is colored blue, the C-terminal  $\beta$ -strand red, while the disordered region and the loop which connects the two  $\beta$ -strands are colored green.

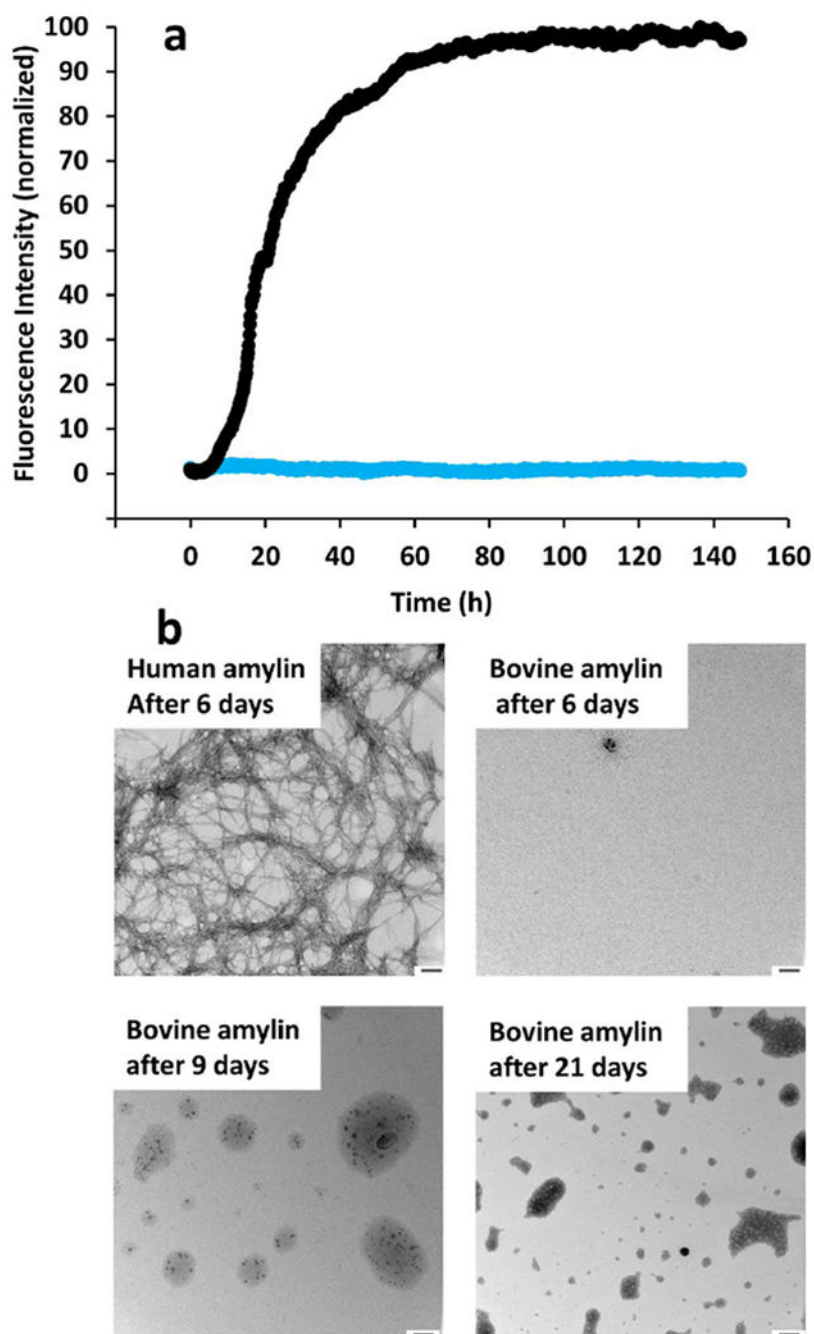


**Figure 2:** Bovine amylin does not form amyloid in Tris buffer. (a) Thioflavin-T fluorescence experiments comparing the kinetics of amyloid formation by human amylin (black) and bovine amylin (blue). (b) TEM images were recorded at different time points. No amyloid formation was observed for bovine amylin for up to 21 days. Experiments were conducted using 16  $\mu$ M peptide, 32  $\mu$ M thioflavin-T at pH 7.4, 25°C and in 20 mM Tris. Scale bar represents 100 nm.

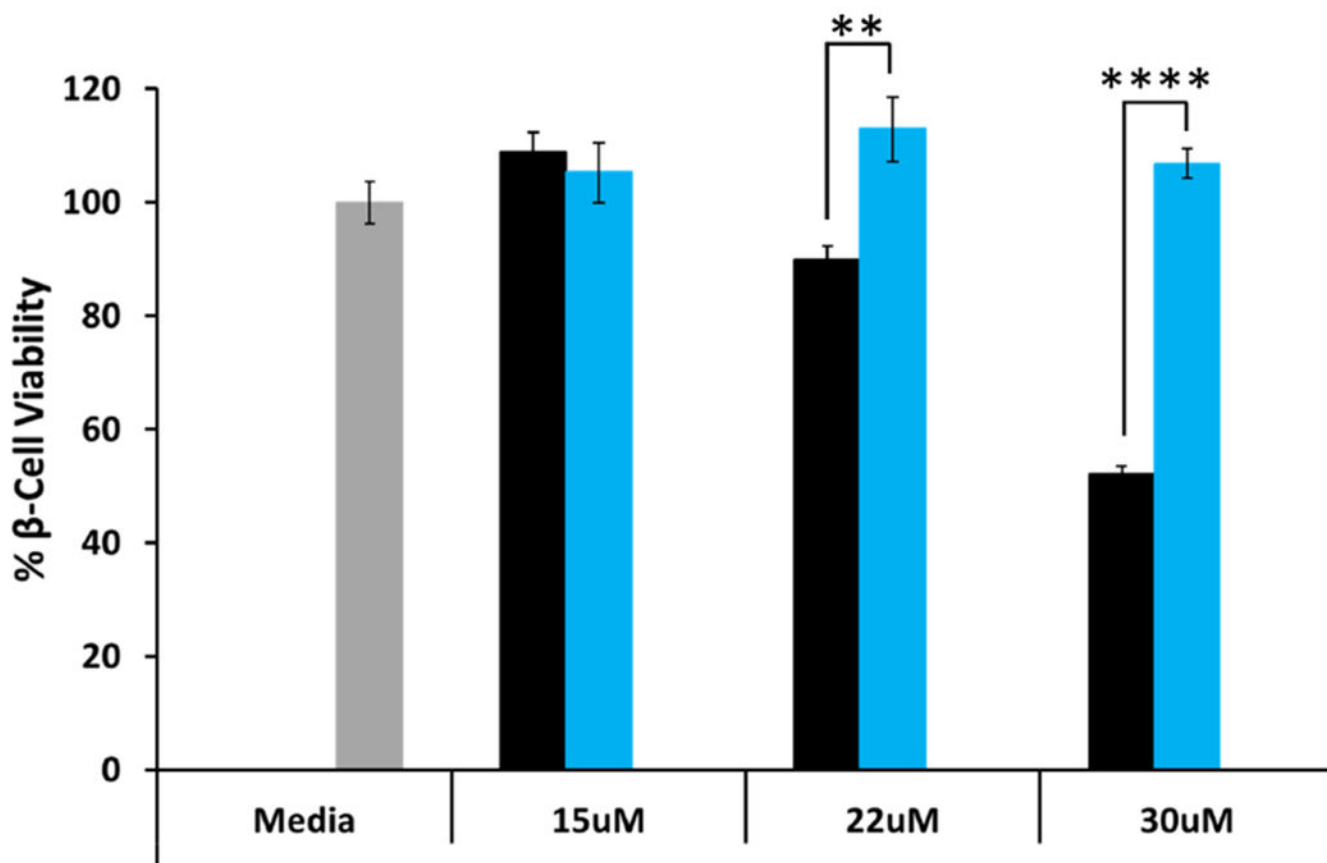


**Figure 3:** Bovine amylin is not toxic to cultured rat INS-1  $\beta$ -cells. The results of 24 h incubation of bovine and human amylin are displayed. Human amylin (black) and bovine amylin (blue) were incubated on rat INS-1  $\beta$ -cells for 24 h and cell viability assessed using Alamar Blue assays. Final peptide concentrations were 15 $\mu$ M, 22  $\mu$ M and 30 $\mu$ M. Data are normalized to cells treated with media (gray). Error bars represent the standard deviation of 3 independent measurements. \*\*P < 0.01, \*\*\*\*P < 0.0001 (Students *t*-test)

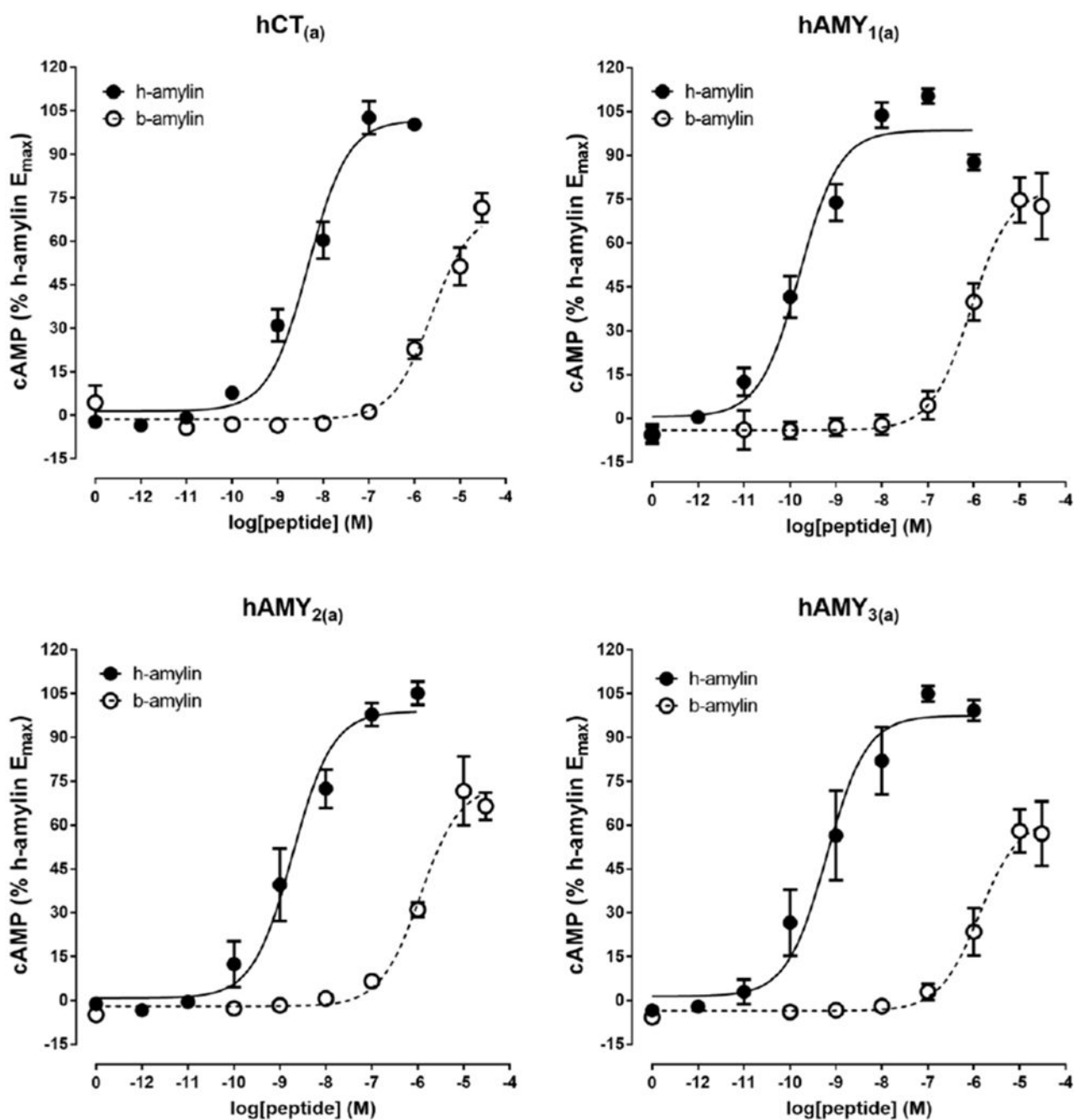


**Figure 4:** Bovine amylin exhibits reduced potency at human amylin receptors. Concentration-response curves of cAMP production by h-amylin compared with b-amylin at hCT<sub>(a)</sub>, hAMY<sub>1(a)</sub>, hAMY<sub>2(a)</sub> and hAMY<sub>3(a)</sub> receptors expressed in Cos-7 cells. Curves are plotted as a percentage of maximal h-amylin stimulated cAMP production and data points are the mean  $\pm$  SEM from at least 3 independent experiments.

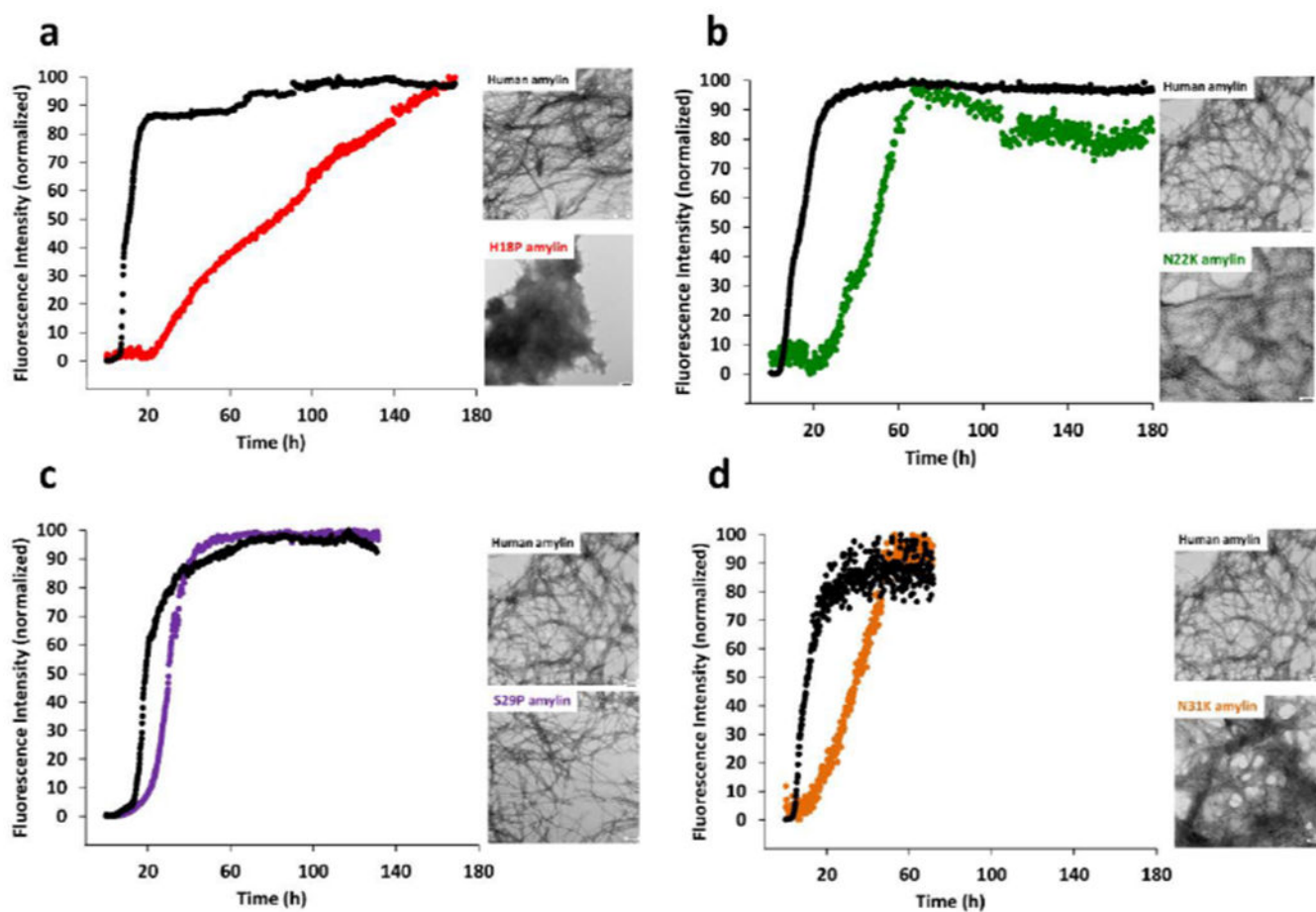


**Figure 5:** Mutational analysis of amyloid formation by human amylin reveals the importance of non-conservative substitutions in modulating amyloidogenicity. Thioflavin-T fluorescence experiments comparing the kinetics of amyloid formation by wildtype h-amylin (black) and (a) H18P h-amylin (red); (b) N22K h-amylin (green); (c) S29P h-amylin (purple) and (d) N31K h-amylin (brown). Data are individually normalized relative to their final maximum fluorescence intensity. Un-normalized data are shown in supporting figure S8. TEM images were collected at the end of the kinetics experiment. Experiments were conducted using 16  $\mu\text{M}$  peptide, 32  $\mu\text{M}$  thioflavin-T at pH 7.4, 25°C and in 20 mM Tris. Scale bars represent 100 nm.

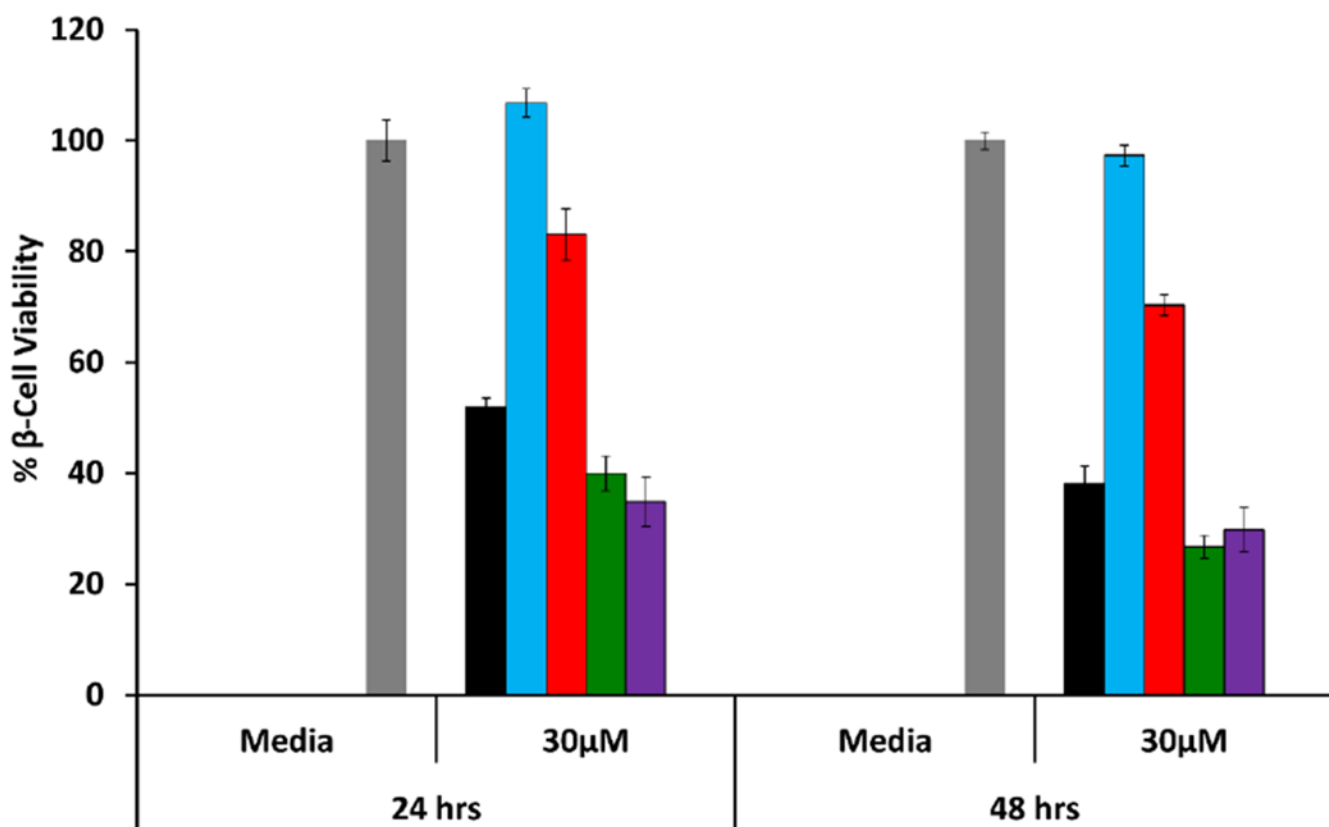


**Figure 6:** Mutational analysis of the reduced  $\beta$ -cell toxicity by bovine amylin. The effects of incubating H18P h-amylin (red), N22K h-amylin (green), S29P h-amylin (purple), human amylin (black), and bovine amylin (blue) on rat INS-1  $\beta$ -cells at 30  $\mu$ M concentration for 24 h and 48 h. Cell viability measured using Alamar Blue assays. Data are normalized relative to cells treated with media (gray).

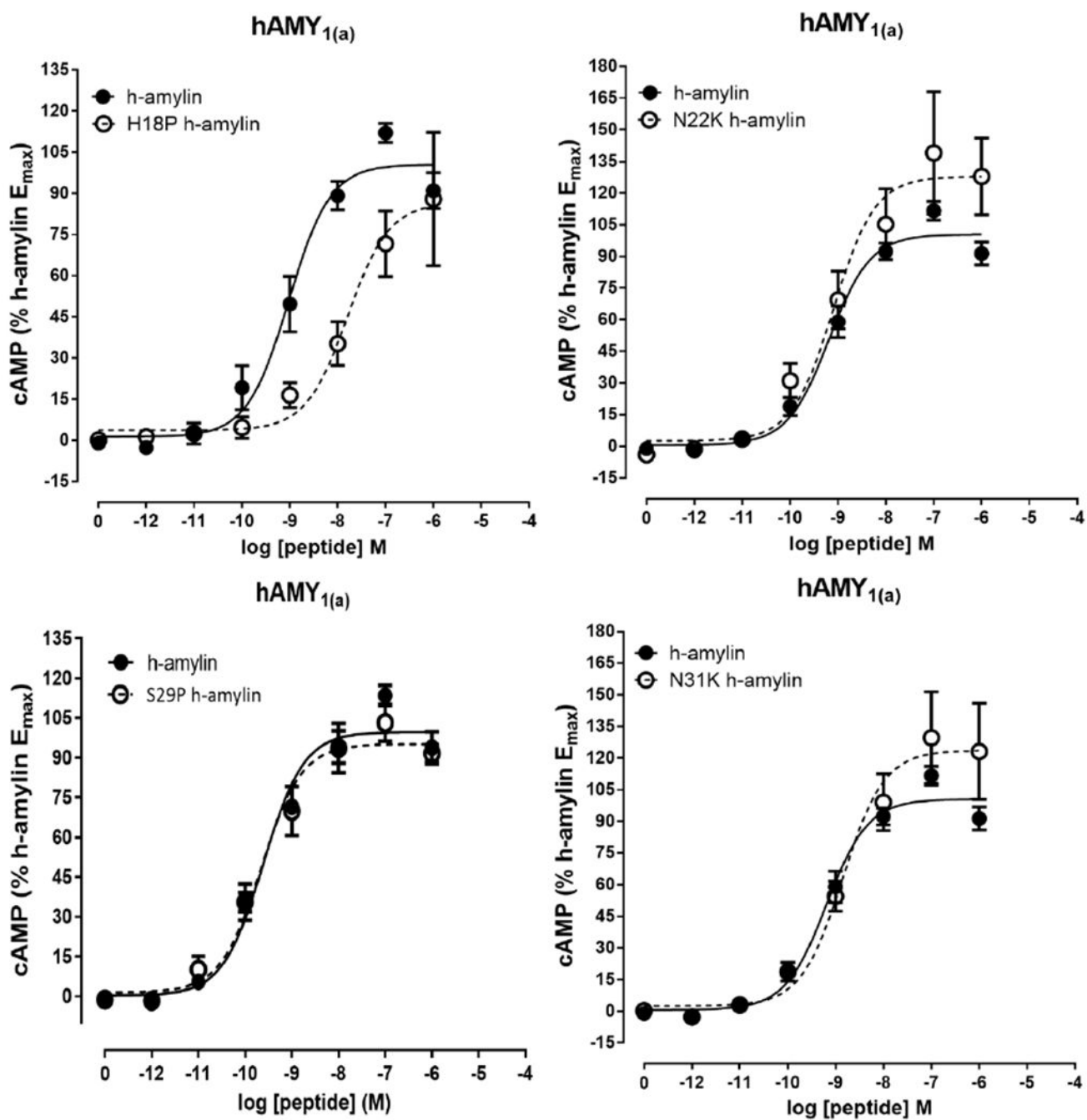


**Figure 7:** Concentration-response curves of cAMP production by h-amylin compared with h-amylin analogs with single-residue substitutions from the b-amylin sequence at the hAMY<sub>1(a)</sub> receptor expressed in Cos-7 cells. Curves are plotted as a percentage of maximal h-amylin stimulated cAMP production and data points represent the mean  $\pm$  SEM from 3-6 independent experiments.

**Table 1:**

Summary of activity data for WT h-amylin and b-amylin including pEC<sub>50</sub> and E<sub>max</sub> values at the hCT<sub>(a)</sub>, hAMY<sub>1(a)</sub>, hAMY<sub>2(a)</sub> and hAMY<sub>3(a)</sub> receptors.

		pEC <sub>50</sub>	Fold-change	n	E <sub>max</sub>	n
hCT <sub>(a)</sub>	h-amylin	8.43 ± 0.16	> -400	7	100	7
	b-amylin	5.81 ± 0.11 ***			62.9 ± 8.25 ***	
hAMY <sub>1(a)</sub>	h-amylin	9.76 ± 0.20	> -5000	7	100	7
	b-amylin	6.04 ± 0.11 ***			83.1 ± 10.6	
hAMY <sub>2(a)</sub>	h-amylin	8.73 ± 0.31	> -600	3	100	3
	b-amylin	5.93 ± 0.04 ***			73.9 ± 4.27 **	
hAMY <sub>3(a)</sub>	h-amylin	9.17 ± 0.45	> -2000	3	100	3
	b-amylin	5.87 ± 0.10 **			62.4 ± 9.31 *	

\* p < 0.05

\*\* p < 0.01

\*\*\* p < 0.001 by unpaired t-test compared to WT h-amylin.